DISCUSSION

After a great success of Imatinib in the treatment of chronic myelogenous leukemia (CML) and gastrointestinal stromal tumors (GISTs), many scientists and industries have been focusing on the development of drugs targeting on cancer-specific molecules[27]. Protein kinases are considered as attractive therapeutic targets for development of anti-cancer drugs because they play critical roles in growth-signaling pathways in cancer cells[28-31]. However, development of an inhibitor(s) which specifically suppresses target kinase activity is not so easy because most of kinase inhibitors are type 1 inhibitor which recognizes an ATP-pocket highly conserved across kinases and competes with ATP. These structural conservation leads to the unexpected cross-reactivity, in some cases yielding unexpected and unfavorable side effects[28, 32]. For discovering new kinase inhibitors with high effectiveness and minimum toxicity, the combination of identification of appropriate target molecules coupled with advanced drug-development tools including analogue synthesis, structure-informed design and fragment-based assembly is essential[28, 33].

To develop MELK-specific inhibitors in this study, we conducted the high-throughput screening for identification of hit compounds and subsequent intensive structure-activity informed study, and finally developed OTSSP167 which effectively inhibited the MELK kinase activity with IC_{50} of 0.41 nM. We then investigated the effect of OTSSP167 on the formation of mammosphere, one of the characteristics of breast cancer stem cells since MELK was reported as a key molecule for cancer stem-cell formation/maintenance[13]. Our results showed that OTSSP167 inhibited mammosphere formation in a dose-dependent manner and also revealed strong growth-suppressive effect on various types of human cancer xenograft including breast, pancreas, prostate and lung cancers without no or a little body-weight loss at the effective doses. The experiment using the MELK-negative cancer cells supported the MELK-dependent growth suppressive effect of OTSSP167 on cancer cells.

In parallel, to further characterize biological mechanisms of the MELK-signaling pathway and verify the mode of action of the MELK inhibitor OTSSP167, we screened novel MELK substrates and identified two possible candidate molecules, DBNL and PSMA1. DBNL is a member of the debrin/Abp1 family of actin-binding proteins and is a component of the immunological synapse that regulates T-cell activation[34]. Although there was no evidence of DNBL involvement in human carcinogenesis, our data have indicated that the phosphorylation of DBNL by MELK is likely to promote cancer cell invasiveness, and probably lead to tumor recurrence and poor prognosis[35]. We also found that MELK could phosphorylate Ser269 on DBNL. Since the phosphrylation of this site was reported to be critical to bind to 14-3-3 proteins[36] that has important roles in the regulation of numerous cellular signaling pathways like cell cycle regulation or apoptosis[37], we suspect that MELK might promote cell growth and mobility of cancer cells through the regulation of the DBNL-14-3-3 signaling pathway.

The other substrate, PSMA1, is one of the components of the 20S core structure of proteasome complex that is important to regulate the concentration of intracellular proteins and remove misfolded proteins through degrading them[38]. The function of PSMA1 itself was not well understood, however, its phosphorylation might affect the assembly of the proteasome complex[39]. A recent study suggested that enhancement of the proteasome assembly and activity could play crucial roles in the maintenance of human embryonic stem cells[40]. We also investigated the biological characteristics of PSMA1 in cancer cells, and found that PSMA1 was stabilized by the phosphorylation in MELK overexpressing

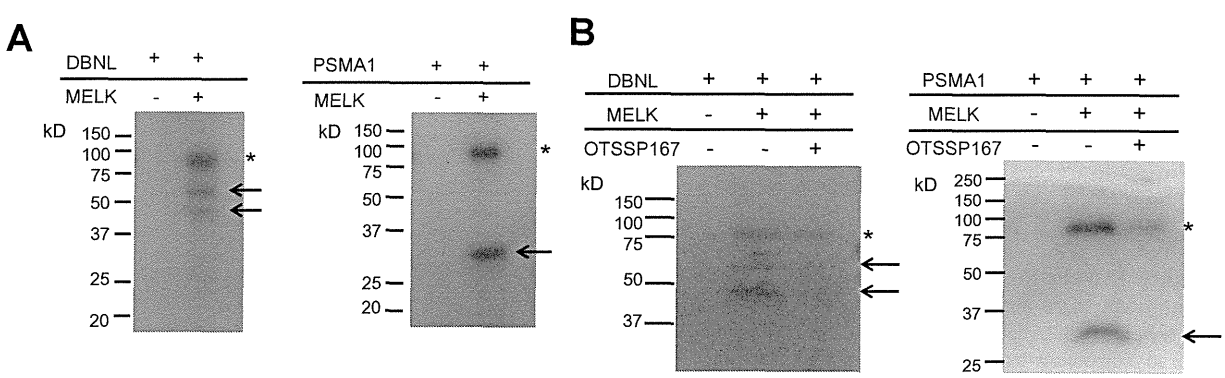

Figure 4: Identification and functional analysis of MELK substrates in breast cancer cell lines. (A) *In vitro* kinase assay using recombinant proteins confirmed DBNL and PSMA1 to be novel substrates of MELK. Arrows indicate phosphorylated substrate proteins; asterisks indicate autophosphorylated MELK. (B) *In vitro* kinase assay using OTSSP167. DBNL (55kDa) or PSMA1 (30kDa) recombinant protein was incubated with MELK with or without OTSSP167. Asterisks indicate autophosphorylated MELK; arrows indicate phosphorylated substrates. Phopshorylation of each substrate was diminished by addition of 10 nM of OTSSP167

cells and that coexistence of PSMA1 and MELK enhanced the formation of mammosphere. Interestingly, the number of mammosphere was significantly decreased in the cells in which PSMA1 expression was knocked down by siRNA for PSMA1. Our data imply that OTSSP167 possibly suppressed mammosphere formation through the reduction of PSMA1 protein.

In summary, we have demonstrated that MELK plays crucial roles in cancer progression and/or stem cell maintenance through phosphorylation of its substrate proteins. Our data have also indicated that that the selective MELK inhibitor OTSSP167 could suppress the phosphorylation of these two MELK substrates, and has the *in vitro* and *in vivo* growth suppressive effect on cancer cells, implicating a great potential of this MELK inhibitor to apply to treatment of various types of human cancer.

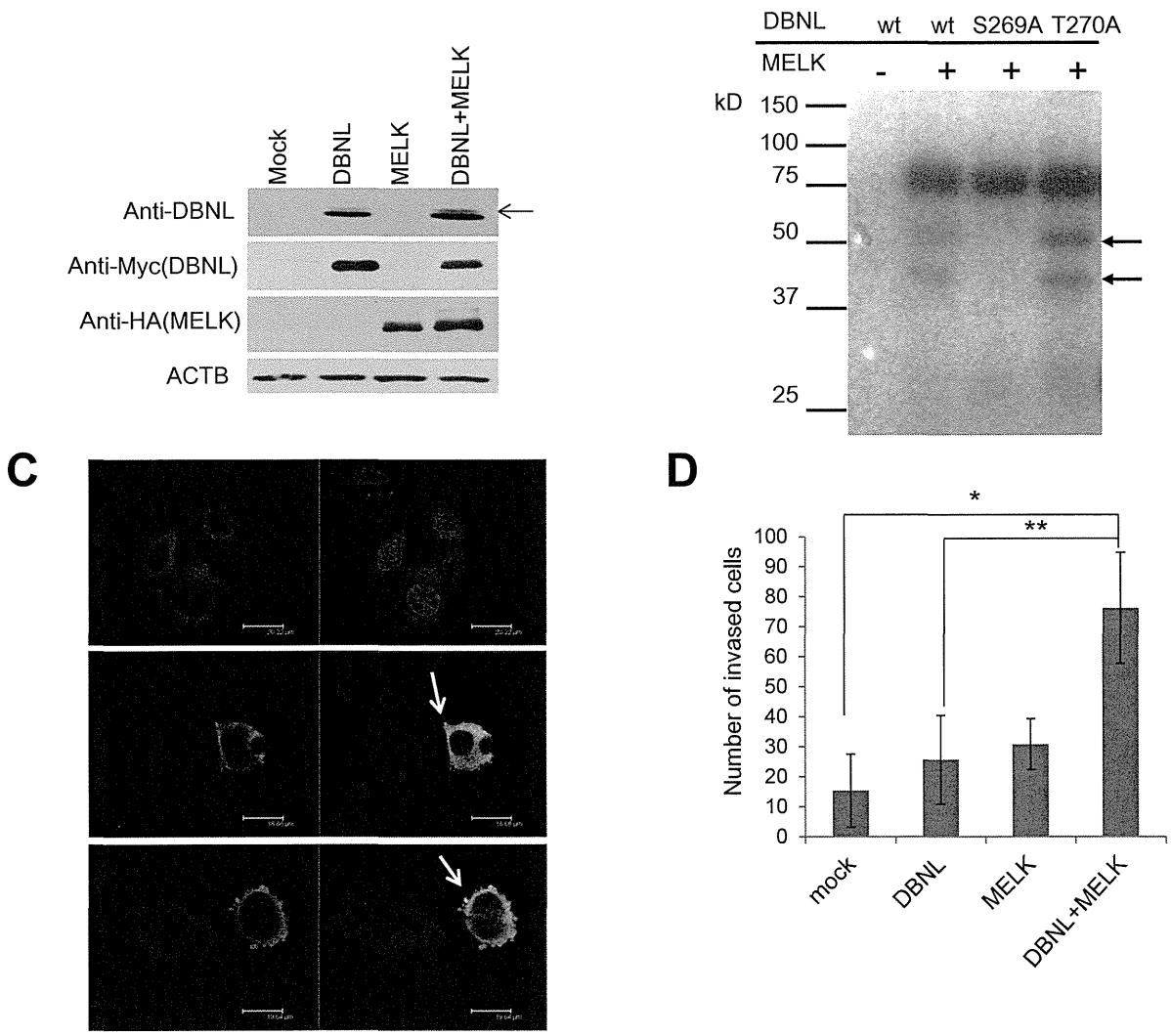

Figure 5: MELK phosphorylated Ser269 on DBNL and induced the cellular invasiveness. (A) *In vivo* phosphorylation assay. Phosphorylation of DBNL (indicated by an arrow) in BT549 cells in which DBNL and MELK were co-transfected was enhanced much stronger than that in the cells in which only DBNL was transfected. (B) Identification of phosphorylated sites by *in vitro* kinase assay. Amino acid substituted mutants of DBNL were generated and used for *in vitro* kinase assay. Phosphorylated band of DBNL in which a serine 269 was substituted with an alanine (S269A) was completely diminished, while that of DBNL in which a threonine 270 was substituted with an alanine (T270A) was unchanged. wt; wild-type. Closed arrows indicate phosphorylated DBNL. (C) Immunocytochemical analysis of cells overexpressing DBNL with/without MELK. MCF-7 cells in which both MELK and DBNL were over-expressed shows a strongly enhanced membrane-ruffling pattern (Red; DBNL, Green; MELK, Blue; DAPI) which is indicated by white arrow. (D) MCF-7 cells over-expressing DBNL revealed elevated cell invasiveness in the presence of MELK. The number of invaded cells on Y-axis indicates the average cell number of migration, that was counted by microscopic observation (*$p=0.009$, **$p=0.0209$, student's t-test). Error bars represent means ± SD of triplicates.

METHODS

High-throughput screening

A library consisting of 108,269 compounds (AMRI's Diverse AMRI Synthetic Library (DASL)) was screened using the assay protocol optimized for the high-throughput low-volume 384-well format assays. Each of the compounds (30 μM) in 342 library plates were incubated for 120 min at room temperature, with 70 μM of ATP, 100 nM of the substrate peptide, and 30 nM of MELK protein. Any plate that showed Z'<0.5 was retested (more details in Supplementary Methods).

Cell lines, plasmids, oligo siRNAs and transfection

MCF-7, MDA-MB-231, BT549, T47D, DU4475, 22Rv1, DU145, HT1197, and NIH3T3 cells were purchased from the American Type Culture Collection (ATCC) (Rockville, MD, USA). A549, PC-14, and MIAPaCa-2 cells were purchased from European Collection of Cell Cultures (ECACC) (Salisbury, UK), RIKEN BioResource Center (Tsukuba, Japan), and Japanese Collection of Research Bioresources Cell Bank (JCRB) (Suita, Japan), respectively. All cells were cultured under appropriate media recommended by suppliers with 10% FBS and 1% antibiotic-antimycotic solution (Sigma-Aldrich). All cells except MDA-MB-231 were maintained at 37 °C in humidified air with 5% CO_2. MDA-MB-231 was maintained at 37 °C in humidified air without CO_2.

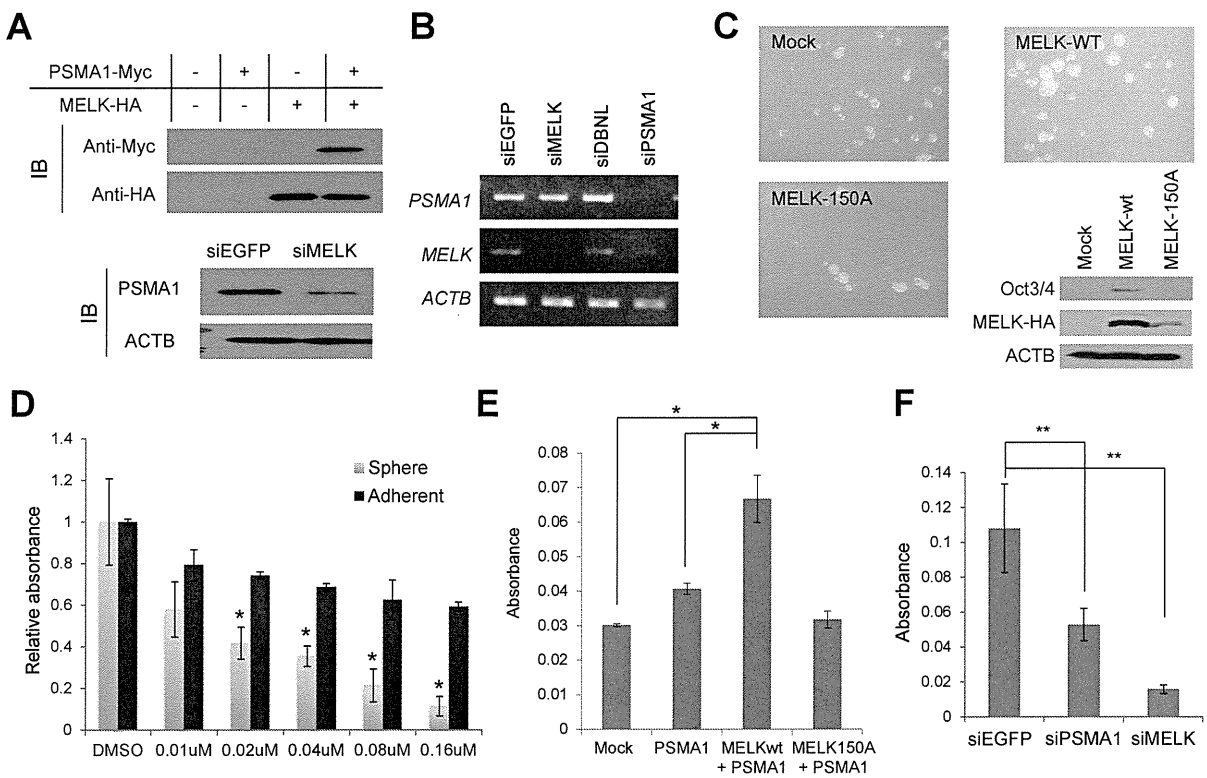

Figure 6: PSMA1 enhanced the mammosphere formation through the phosphorylation by MELK. (A, B) PSMA1 protein was stabilized through the phosphorylation by MELK in breast cancer cells (A) although transcriptional level of PSMA1 was unchanged in the cells in which MELK expression was knocked down (B). (C) Wild-type MELK (MELK-wt) or kinase-dead mutant MELK (MELK-150A) expression vector was transfected into MCF-7 cells which were seeded onto an ultra-low attachment culture plate. The formation of mammosphere was enhanced in cells in which MELK-wt was transiently introduced than those transfected with mock vector or MELK-150A. The expression levels of one of cancer stem cell markers, Oct3/4, are shown. The cells which transiently over-expressed MELK-wt induced Oct3/4 expression while those transfected with mock vector or MELK-150A revealed no Oct3/4 expression. (D) OTSSP167 suppressed more significantly the formation of mammosphere than the growth of attached MCF-7 cells. The cells were plated onto ultra-low attachment culture plate or normal culture plate without or with OTSSP167 of given concentrations (*$p<0.05$, student's t-test). (E) The MCF-7 cells in which both PSMA1 and wild-type MELK (MELK wt) were co-overexpressed revealed higher number of mammosphere formation than the parental MCF-7 cells or those transfected with PSMA1 alone or PSMA1 + kinase-dead MELK (MELK D150A) (*$p<0.0001$, student's t-test). (F) The mammosphere formation of MDA-MB-231 cells, in which PSMA1 was knocked down, was suppressed (**$p<0.05$, student's t-test). Absorbance measured at 490 nm is indicated using that at 630 nm as a reference with a microplate reader. Error bars represent means ± SD of triplicates for experiments D-F.

MELK wild-type and kinase-dead mutant (D150A) plasmids were constructed previously[9]. To construct vectors designed to express DBNL (NM_001014436.2) or PSMA1 (NM_002786.3), the entire coding sequences were amplified by RT-PCR and cloned into the pcDNA3.1-myc-his or pCAGGSnHc expression vector. We carried out site-directed mutagenesis PCR to generate DBNL substituted mutants (S269A and T270A) with a QuickChange site-directed Mutagenesis kit (Stratagene). Plasmids were transfected using Fugene6 (for NIH3T3) or FugeneHD (for human breast cancer cell lines) (Roche) according to the supplier's recommendations. For knockdown experiments, cells were transfected with oligo siRNA using Lipofectamine RNAiMAX (Invitrogen) according to manufacturer's instructions. The target sequences of oligo siRNAs were as follows: 5'-GACAUCCUAUCUAGCUGCA-3' for MELK; 5'-CAGAUACCAACACAACGAU-3' for PSMA1; 5'-GGTGCTGGCTCTGAGCACA-3' for DBNL; 5′-TTGAAGCAGCACGACUUCUUC-3′ and 5′-TTGAAGAAGUCGUGCUGCUUC-3′ for siEGFP.

Recombinant proteins and in vitro kinase assay for substrate screening

MELK recombinant protein was generated as described previously[9]. The full coding sequence of each of MELK substrate candidates was amplified by RT-PCR and cloned into the pGEX6p-1 vector (GE Healthcare). The GST-tagged recombinant proteins were expressed in BL21 codon-plus RIL competent cells (Stratagene) and purified using Glutathione Sepharose 4B beads (GE Healthcare) according to the supplier's instructions. The GST-tag was removed by PreScission protease (GE Healthcare) according to the supplier's instructions. For *in vitro* kinase assay, MELK recombinant protein (0.4 μg) was mixed with 5 μg of each substrate in 20 μl of kinase buffer containing 30 mM Tris-HCl (pH), 10 mM DTT, 40 mM NaF, 10 mM $MgCl_2$, 0.1 mM EGTA with 50 μM cold-ATP and 10 Ci of [γ-^{32}P]ATP (GE Healthcare) for 30 min at 30 °C. The reaction was terminated by addition of SDS sample buffer and boiled for 5 min prior to SDS-PAGE. The gel was dried and autoradiographed with intensifying screens at room temperature. OTSSP167 (final concentration of 10 nM) was dissolved in DMSO and added to kinase buffer before the incubation.

Western blot analysis and immunocytochemistry

Cells were lysed with RIPA buffer containing protease inhibitor cocktail and phosphatase inhibitor cocktail (Calbiochem). The proteins were separated by electrophoresis using 10% or 7.5% SDS-PAGE gel and transferred onto nitrocellulose membrane. The membranes were incubated with the first antibody, respectively: anti-PSMA1 antibody (Epitomics), anti-DBNL antibody, anti-Myc (Santa Cruz Biothechnology), anti-HA (Roche), anti-Oct3/4 (Santa Cruz Biothechnology) or anti-ACTB. We generated mouse anti-MELK monoclonal antibodies using partial recombinant MELK protein (264-601 amino acids of MELK) as an immunogen by the methods as described previously[41]. For immunocytochemistry, MCF-7 cells were seeded onto glass slide-chamber and transfected with expression vector(s) as described above. After 48 hours of incubation, cells were fixed with 4% paraformaldehyde and permeabilized with 0.1% Triton X-100 in PBS for 1 min at room temperature. Non-specific binding was blocked by treatment with PBS containing 3% bovine serum albumin (BSA) for 30 min at room temperature. Cells were incubated for 60 min at room temperature with anti-HA or anti-DBNL antibody diluted at 1:200 by PBS containing 3% BSA. After washing with PBS, cells were stained by Alexa fluor-conjugated secondary antibody (Invitrogen) for 60 min at room temperature, and visualized with Spectral Confocal Scanning Systems (Leica).

In vivo phosphorylation assay

DBNL expression vector was transfected into cells with or without MELK expression vector. After 48 hours of incubation, cells were treated with 100 nM Okadaic acid (Calbiochem) and incubated for 6 hours. The cells were lysed after the treatment with Okadaic acid and the lysed samples were loaded into 7.5% SDS-PAGE gel. The proteins were transferred onto nitrocellulose membrane (GE Healthcare). The membrane was incubated with anti-DBNL antibody (Abnova) or anti-β-actin (ACTB) (Sigma-Aldrich). ACTB served as a loading control.

Matrigel invasion assay and mammosphere formation assay

NIH3T3 cells transfected with plasmids expressing MELK (pCAGGSnHc-MELK), DBNL (pcDNA3.1-Myc-His-DBNL) or both were grown to near confluence in DMEM containing 10% FBS. After the incubation of 24 hours, the cells were harvested by trypsinization, washed in DMEM without addition of serum, and suspended in serum-free DMEM. The cells ($1x10^4$ cells) were seeded onto the Matrigel matrix chamber (BD Biosciences) and incubated for 22 hours.The cells invading to Matrigel were stained by Giemsa (Merck) and counted. For sphere formation assay, $1x10^3$ cells of MCF-7 cells which transiently over-expressed wild-type MELK, kinase-dead MELK, PMSA1, PSMA1 and wild-type MELK, or PMSA and kinase-dead MELK were seeded onto Ultra-Low attachment plate (Corning). For knockdown experiments, MDA-MB-231 cells ($1x10^3$ cells) which seeded onto Ultra-Low attachment plate were transfected with oligo siRNA for EGFP, MELK or PSMA1 as described above. For examination of sphere formation under treatment of MELK inhibitor OTSSP167, $1x10^3$ MCF-7 cells were seeded with 0.01, 0.02, 0.04, 0.08, or 0.16 μM of OTSSP167, respectively. DMSO alone was used as a control. Following incubation for two weeks, cell viability was measured by using Cell-counting kit-8 (DOJINDO).

In vivo xenograft study

MDA-MB-231 cells were injected into the mammary fat pads of NOD.CB17-*Prkdc*^{scid}/J mice (Charles River Laboratory). A549, MIAPaCa-2 and PC-14 cells (1 x 10^7 cells) were injected subcutaneously in the left flank of female BALB/cSLC-nu/nu mice (Japan SLC, Inc.). DU145 cells were injected subcutaneously in the left flank of male BALB/cSLC-nu/nu mice (Japan SLC, Inc.). When MDA-MB-231, A549, DU145, MIAPaCa-2, and PC-14 xenografts had reached an average volume of 100, 210, 110, 250, and 250 mm^3, respectively, animals were randomized into groups of 6 mice (except for PC-14, for which groups of 3 mice were used). For oral administration, compounds were prepared in a vehicle of 0.5% methylcellulose and given by oral garbage at the indicated dose and schedule. For intravenous administration, compounds were formulated in 5% glucose and injected into the tail vein. An administration volume of 10 ml per kg of body weight was used for both administration routes. Concentrations were indicated in main text and Figures. Tumor volumes were determined every other day using a caliper. The results were converted to tumor volume (mm^3) by the formula length x $width^2$ x 1/2. The weight of the mice was determined as an indicator of tolerability on the same days. The animal experiments using A549 xenografts were conducted by contract with KAC Co., Ltd. (Shiga, Japan) in accordance with their Institutional Guidelines for the Care and Use of Laboratory Animals. The other animal experiments were conducted at OncoTherapy Science, Inc. in accordance with their Institutional Guidelines for the Care and Use of Laboratory Animals. Tumor growth inhibition (TGI) was calculated according to the formula $\{1 - (T - T_0) / (C - C_0)\} \times 100$, where T and T_0 are the mean tumor volumes at day 14 and day 0, respectively, for the experimental group, and $C - C_0$ are those for the vehicle control group.

Statistical analysis

All values were presented as means ± SD. Statistical significance was computed using student's t-test, and the level of significance was set at $p<0.05$.

Detailed methods are described in the Supplementary Methods.

ACKNOWLEDGMENTS

We thank S. Hisada for *in vitro* experimental designs for the inhibitor discovery and manuscript preparation, and K. Toyota for technical support in *in vitro* experiments on compounds. This work was supported in part by the Innovation Promotion Program of the New Energy and Industrial Technology Development Organization (NEDO) of Japan.

Author contributions

Y.N. planned and supervised the entire project; Y.N. and S.C. designed the study for identification of MELK substrate and functional analysis; S.C. performed most of the experiments and summarized the functional analysis results; S.C and K.K. performed subcloning and protein purification; A.T. and K.U performed mass spectrometry; Y.M. contributed to the planning of the novel MELK inhibitor discovery research and the compound design; H.S. and T.M. performed *in vitro* experiments and data analyses for the inhibitor discovery; N.T. performed *in vivo* xenograft studies; S.C., Y.N. and Y.M wrote the manuscript; Y.N obtained funding for the study.

Competing Interests

H.S., T.M., N.T., and Y.M. are employees of OncoTherapy Science, Inc. Y.N. is a stock holder and a scientific advisor of OncoTherapy Science, Inc. The other authors declare no competing interests.

REFERENCE

1. Jemal A, Siegel R, Ward E, Hao Y, Xu J, Murray T, Thun MJ. Cancer statistics, 2008. CA Cancer J Clin. 2008; 58:71-96.
2. Forouzanfar MH, Foreman KJ, Delossantos AM, Lozano R, Lopez AD, Murray CJ, Naghavi M. Breast and cervical cancer in 187 countries between 1980 and 2010: A systematic analysis. Lancet. 2011; 378:1461-1484.
3. Sotiriou C, Pusztai L. Gene-expression signatures in breast cancer. N Engl J Med. 2009; 360:790-800.
4. Rakha EA, Elsheikh SE, Aleskandarany MA, Habashi HO, Green AR, Powe DG, El-Sayed ME, Benhasouna A, Brunet JS, Akslen LA, Evans AJ, Blamey R, Reis-Filho JS, Foulkes WD, Ellis IO. Triple-negative breast cancer: Distinguishing between basal and nonbasal subtypes. Clin Cancer Res. 2009; 15:2302-2310.
5. Griffiths CL, Olin JL. Triple negative breast cancer: A brief review of its characteristics and treatment options. J Pharm Pract. 25:319-323.
6. Cleator S, Heller W, Coombes RC. Triple-negative breast cancer: Therapeutic options. Lancet Oncol. 2007; 8:235-244.
7. Foulkes WD, Smith IE, Reis-Filho JS. Triple-negative breast cancer. N Engl J Med. 2010; 363:1938-1948.
8. Heyer BS, Warsowe J, Solter D, Knowles BB, Ackerman SL. New member of the snf1/ampk kinase family, melk, is expressed in the mouse egg and preimplantation embryo. Mol Reprod Dev. 1997; 47:148-156.
9. Lin ML, Park JH, Nishidate T, Nakamura Y, Katagiri T. Involvement of maternal embryonic leucine zipper kinase (melk) in mammary carcinogenesis through interaction with

bcl-g, a pro-apoptotic member of the bcl-2 family. Breast Cancer Res. 2007; 9:R17.

10. Gray D, Jubb AM, Hogue D, Dowd P, Kljavin N, Yi S, Bai W, Frantz G, Zhang Z, Koeppen H, de Sauvage FJ, Davis DP. Maternal embryonic leucine zipper kinase/ murine protein serine-threonine kinase 38 is a promising therapeutic target for multiple cancers. Cancer Res. 2005; 65:9751-9761.
11. Bianchini G, Iwamoto T, Qi Y, Coutant C, Shiang CY, Wang B, Santarpia L, Valero V, Hortobagyi GN, Symmans WF, Gianni L, Pusztai L. Prognostic and therapeutic implications of distinct kinase expression patterns in different subtypes of breast cancer. Cancer Res. 2010; 70:8852-8862.
12. Sutter R, Yadirgi G, Marino S. Neural stem cells, tumour stem cells and brain tumours: Dangerous relationships? Biochim Biophys Acta. 2007; 1776:125-137.
13. Hebbard LW, Maurer J, Miller A, Lesperance J, Hassell J, Oshima RG, Terskikh AV. Maternal embryonic leucine zipper kinase is upregulated and required in mammary tumor-initiating cells in vivo. Cancer Res. 2010; 70:8863-8873.
14. Rich JN. Cancer stem cells in radiation resistance. Cancer Res. 2007; 67:8980-8984.
15. Dean M, Fojo T, Bates S. Tumour stem cells and drug resistance. Nat Rev Cancer. 2005; 5:275-284.
16. Kemper K, Grandela C, Medema JP. Molecular identification and targeting of colorectal cancer stem cells. Oncotarget. 2010; 1:387-395.
17. Curtin JC, Lorenzi MV. Drug discovery approaches to target wnt signaling in cancer stem cells. Oncotarget. 2010; 1:563-577.
18. Nakano I, Masterman-Smith M, Saigusa K, Paucar AA, Horvath S, Shoemaker L, Watanabe M, Negro A, Bajpai R, Howes A, Lelievre V, Waschek JA, Lazareff JA, Freije WA, Liau LM, Gilbertson RJ, et al. Maternal embryonic leucine zipper kinase is a key regulator of the proliferation of malignant brain tumors, including brain tumor stem cells. J Neurosci Res. 2008; 86:48-60.
19. Sportsman JR, Gaudet EA, Boge A. Immobilized metal ion affinity-based fluorescence polarization (imap): Advances in kinase screening. Assay Drug Dev Technol. 2004; 2:205-214.
20. Larbolette O, Wollscheid B, Schweikert J, Nielsen PJ, Wienands J. Sh3p7 is a cytoskeleton adapter protein and is coupled to signal transduction from lymphocyte antigen receptors. Mol Cell Biol. 1999; 19:1539-1546.
21. Mise-Omata S, Montagne B, Deckert M, Wienands J, Acuto O. Mammalian actin binding protein 1 is essential for endocytosis but not lamellipodia formation: Functional analysis by rna interference. Biochem Biophys Res Commun. 2003; 301:704-710.
22. Kessels MM, Engqvist-Goldstein AE, Drubin DG, Qualmann B. Mammalian abp1, a signal-responsive f-actin-binding protein, links the actin cytoskeleton to endocytosis via the gtpase dynamin. J Cell Biol. 2001; 153:351-366.
23. Cohen P, Holmes CF, Tsukitani Y. Okadaic acid: A new probe for the study of cellular regulation. Trends Biochem Sci. 1990; 15:98-102.
24. Yamaguchi K, Hata K, Wada T, Moriya S, Miyagi T. Epidermal growth factor-induced mobilization of a ganglioside-specific sialidase (neu3) to membrane ruffles. Biochem Biophys Res Commun. 2006; 346:484-490.
25. Deng S, Zhou H, Xiong R, Lu Y, Yan D, Xing T, Dong L, Tang E, Yang H. Over-expression of genes and proteins of ubiquitin specific peptidases (usps) and proteasome subunits (pss) in breast cancer tissue observed by the methods of rfdd-pcr and proteomics. Breast Cancer Res Treat. 2007; 104:21-30.
26. He X, Gonzalez V, Tsang A, Thompson J, Tsang TC, Harris DT. Differential gene expression profiling of cd34+ cd133+ umbilical cord blood hematopoietic stem progenitor cells. Stem Cells Dev. 2005; 14:188-198.
27. Zhang Z, Stiegler AL, Boggon TJ, Kobayashi S, Halmos B. Egfr-mutated lung cancer: A paradigm of molecular oncology. Oncotarget. 2010; 1:497-514.
28. Zhang J, Yang PL, Gray NS. Targeting cancer with small molecule kinase inhibitors. Nat Rev Cancer. 2009; 9:28-39.
29. Schmidt-Kittler O, Zhu J, Yang J, Liu G, Hendricks W, Lengauer C, Gabelli SB, Kinzler KW, Vogelstein B, Huso DL, Zhou S. Pi3kalpha inhibitors that inhibit metastasis. Oncotarget. 2010; 1:339-348.
30. Liu-Sullivan N, Zhang J, Bakleh A, Marchica J, Li J, Siolas D, Laquerre S, Degenhardt YY, Wooster R, Chang K, Hannon GF, Powers S. Pooled shrna screen for sensitizers to inhibition of the mitotic regulator polo-like kinase (plk1). Oncotarget. 2011; 2:1254-1264.
31. Hantschel O, Grebien F, Superti-Furga G. Targeting allosteric regulatory modules in oncoproteins: «Drugging the undruggable». Oncotarget. 2011; 2:828-829.
32. Crespo A, Zhang X, Fernandez A. Redesigning kinase inhibitors to enhance specificity. J Med Chem. 2008; 51:4890-4898.
33. Morachis JM, Huang R, Emerson BM. Identification of kinase inhibitors that target transcription initiation by rna polymerase ii. Oncotarget. 2011; 2:18-28.
34. Le Bras S, Foucault I, Foussat A, Brignone C, Acuto O, Deckert M. Recruitment of the actin-binding protein hip-55 to the immunological synapse regulates t cell receptor signaling and endocytosis. J Biol Chem. 2004; 279:15550-15560.
35. Friedl P, Locker J, Sahai E, Segall JE. Classifying collective cancer cell invasion. Nat Cell Biol. 2012; 14:777-783.
36. Li X, Wolf ME. Visualization of virus-infected brain regions using a gfp-illuminating flashlight enables accurate and rapid dissection for biochemical analysis. J Neurosci Methods. 2011; 201:177-179.
37. Hermeking H. The 14-3-3 cancer connection. Nat Rev

Cancer. 2003; 3:931-943.

38. Murata S, Yashiroda H, Tanaka K. Molecular mechanisms of proteasome assembly. Nat Rev Mol Cell Biol. 2009; 10:104-115.
39. Bose S, Stratford FL, Broadfoot KI, Mason GG, Rivett AJ. Phosphorylation of 20s proteasome alpha subunit c8 (alpha7) stabilizes the 26s proteasome and plays a role in the regulation of proteasome complexes by gamma-interferon. Biochem J. 2004; 378:177-184.
40. Vilchez D, Boyer L, Morantte I, Lutz M, Merkwirth C, Joyce D, Spencer B, Page L, Masliah E, Berggren WT, Gage FH, Dillin A. Increased proteasome activity in human embryonic stem cells is regulated by psmd11. Nature. 2012; 489:304-308.
41. Fukukawa C, Hanaoka H, Nagayama S, Tsunoda T, Toguchida J, Endo K, Nakamura Y, Katagiri T. Radioimmunotherapy of human synovial sarcoma using a monoclonal antibody against fzd10. Cancer Sci. 2008; 99:432-440.